ACS Photonics

Article

pubs.acs.org/journal/apchd5

Plasmon-Enhanced Whispering Gallery Mode Lasing from Hexagonal Al/ZnO Microcavity

Junfeng Lu, Chunxiang Xu,* Jun Dai, Jitao Li, Yueyue Wang, Yi Lin, and Panlin Li

State Key Laboratory of Bioelectronics, School of Biological Science and Medical Engineering, Southeast University, Nanjing 210096, People's Republic of China

ABSTRACT: Wurtzite structural ZnO microrods with hexagonal cross section were fabricated by a simple vapor transport method and an individual ZnO microrod was employed as a whispering gallery microcavity. The obviously enhanced spontaneous and stimulated emissions were observed as the ZnO microrod was decorated with Al nanoparticles (NPs). Based on the absorption spectrum of Al NPs, the underlying mechanism was proposed and can be attributed to the resonant coupling between excitons of ZnO and surface plasmons (SPs) of Al NPs at the metal/ZnO interface on the surface of microcavity. In addition, the threshold of the ZnO microcavity decorated with Al NPs has reduced by half compared with that of the bare one, which provides additional evidence to support the energy coupling between the ZnO microrod and Al NPs. The controllability and improved emission properties of these types of microcavities are potentially important for designing highly efficient optoelectronic devices.

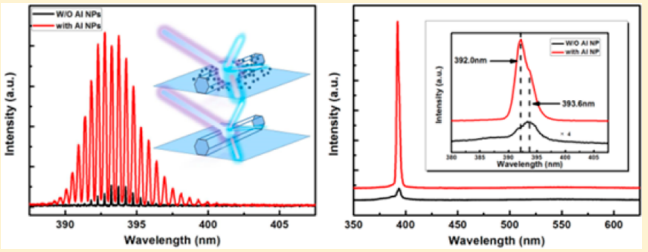

KEYWORDS: *plasmon-enhanced, whispering gallery mode, ZnO microrods, lasing, Al nanoparticles, vapor-phase transport*

Zinc oxide (ZnO), a direct wide bandgap (3.37 eV) semiconductor material with a large exciton binding energy (60 meV), has drawn much attention due to their potential applications in ultraviolet (UV) optoelectronic devices, such as light emitting diodes,[1−4] micro/nanolasers,[5−8] and UV photodetectors.[9−12] Recent progress in lasing or stimulated emission has been achieved from a variety of low-dimensional ZnO micro/nanostructures. The reported stimulated emission process can be summarized in random mode,[8,13] Fabry−Pérot (FP) mode,[5,6] and whispering gallery mode (WGM).[7,14−16] However, both random lasing and FP lasing generally present a high threshold due to the scattering at the disordered ZnO interfaces and the low reflectivity at the two end facets of the 1D ZnO micro/nanostructure. On the other hand, the single-crystal hexagonal ZnO microstructure constitutes a nature WGM microcavity, where the light wave propagates circularly in the inner walls due to multiple total internal reflection at the ZnO/air boundary; therefore, it is expected to obtain UV lasing with high quality factor and low threshold. But now, the luminescence efficiency of ZnO microlaser needs to be improved. In order to enhance spontaneous and stimulated emission from ZnO micro/nanostructures, much attention has been paid on the resonant cavity based on ZnO micro/nanostructures composited with metal NPs, such as Ag,[17,18] Au,[19,20] and Pt.[21] Surface plasmons (SPs), excited by the interaction between light and electron plasma waves at the metal surface, has attracted great scientific interest due to its wide applications, including plasmon lasers,[22] enhancing the light absorption,[23] and Raman scattering[24] of materials near its surface. Recently, SP-mediated emission has also become an attractive research topic because of the dramatic improvement of luminescence intensity and efficiency of light-emitting materials and devices. For example, Zhang et al. reported the enhanced electroluminescence intensity in an n-ZnO/AlN/p-GaN heterojunction light emitting diode resulting from the resonant coupling between excitons in ZnO and localized surface plasmon in Ag NPs.[25]

The metal-decorated WGM microcavity constructs a better configuration that is beneficial for the coupling between the ZnO interband emission and the metal SP because both surface evanescent waves are mainly confined on the microcavity surface, where the former reflects totally and internally,[26] meanwhile, the latter is localized in the metal/ZnO interface. This effective coupling is expected to improve the lasing performance, but few investigations have been reported so far. In this work, more than 10-fold enhancement of the spontaneous and stimulated emission was demonstrated from Al-decorated ZnO microrod, while a slightly blue shift was discovered. Both the enhanced intensity and the blue shift are attributed to the surface plasma resonance (SPR) induced by Al NPs, because the SP energy is very close to the ZnO band gap.[27,28] These results are helpful for the creation of high efficient optoelectronic devices.

RESULTS AND DISCUSSION

Morphology and Structural Characterization. Figure 1a shows a typical scanning electron microscope (SEM) image of the ZnO microrods vertically grown on a silicon substrate. The

Received: July 19, 2014
Published: December 2, 2014

   dx.doi.org/10.1021/ph5002582 | *ACS Photonics* 2015, 2, 73−77

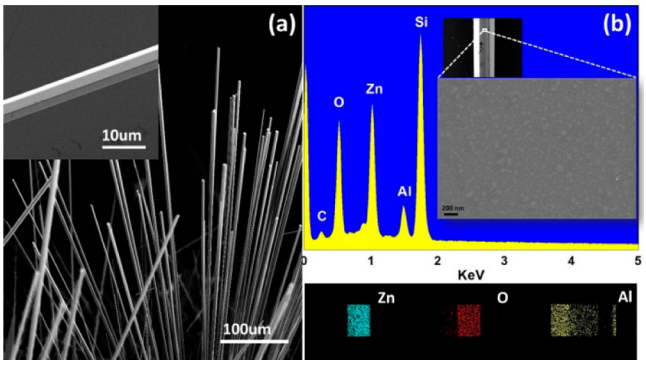

Figure 1. (a) SEM image of the as-grown ZnO microrods inserted with an enlarged individual microrod. (b) EDS spectrum and the Zn, O, and Al element mapping images for the individual ZnO microrod. Inset: SEM image of the Al NPs deposited on the surface of the individual ZnO microrod, taken from the white marked rectangle spot.

length of the ZnO microrods is ~2 mm and the diameter is 10−20 μm. An individual ZnO microrod with a hexagonal cross section and smooth facets as inserted in Figure 1a is selected to act as a WGM lasing microcavity. The EDS spectrum and elemental mapping profiles of the Al-decorated ZnO microrod confirm the existence of Al element, as shown in Figure 1b. The elemental mapping images collected from the rectangular region in Figure 1b reveals that the Zn element and O element distribute uniformly corresponding distinctly to the profile of the ZnO microrod, while the Al element disperses on the surface of the microrod. The SEM image inserted in Figure 1b further demonstrates that the aluminum exists as NPs with diameters of about 60−80 nm.

Optical Property. To examine the optical properties of the ZnO microrod with and without decoration of Al NPs, the μ-PL spectra measurements were performed at room temperature. As shown in Figure 2, the μ-PL spectra from an

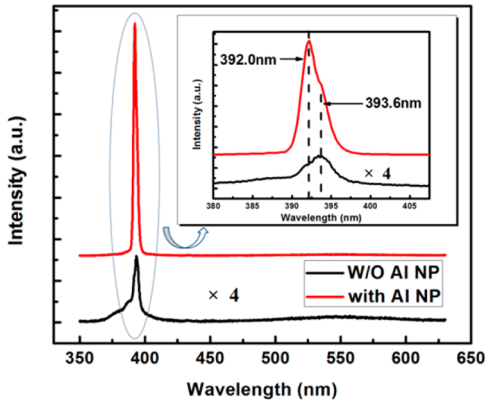

Figure 2. μ-PL spectra of the ZnO microrod before (black line) and after (red line) Al NPs decoration under the same excitation power. Inset: the μ-PL spectra of the two samples in short wavelength region.

individual ZnO microrod before (black line) and after (red line) Al NPs decoration mainly display a UV emission peak centered at 392.5 nm from the near band-edge emission (NBE) of ZnO.[30−32] Under the same experiment condition, the UV emission peak intensity from the Al-decorated ZnO microrod is approximately 10-fold strong as that of the bare ZnO one. In order to investigate the contribution of the SP from Al NPs, the optical absorption spectra of Al NPs prepared at the same sputtering condition, was measured and as inserted in Figure 3. An obvious absorption exists in ZnO NBE region. This

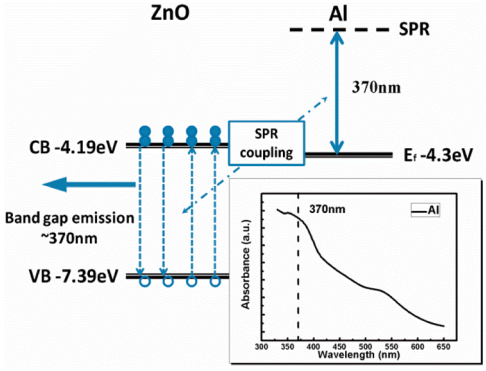

Figure 3. Schematic resonant coupling between ZnO NBE and Al surface plasmon inserted with the absorption spectrum of Al NPs prepared under the same conditions with the decoration on ZnO microrods.

provides an important physical environment for the resonant coupling between ZnO NBE and Al SP. To illustrate the above-mentioned mechanism, the schematic diagram of the band alignment between the ZnO microrod and Al NPs is plotted in Figure 3, in which the conduction band of ZnO is located at −4.19 eV versus the absolute vacuum scale (AVS), and the Fermi level of aluminum is at −4.3 eV versus AVS.[33,34] The strong resonant surface plasmon coupling will give rise to an enhanced interband transition and further results in an enhanced band gap recombination for spontaneous emission and lasing from ZnO microrod. Based on this mechanism, more effective coupling should happen in the short wavelength region because the Al SP presents more and more strong response with the wavelength shortening, as shown the absorption spectrum. Therefore, the blue shift of the NBE emission is observed from the Al-decorated ZnO microrods, as shown in the inset in Figure 2.

The SP-improved WGM lasing performance was also characterized from the ZnO microrod before and after Al NPs decoration under different pumping power, as shown in Figure 4a,b. At a low pumping power of 3.2 μW, the spectrum displays a weak spontaneous emission band centered at 391 nm for the ZnO microrod without Al NPs. When the pumping power reaches to 4.85 μW, some sharp peaks with the mode spacing of about 0.45 nm emerge out. As the pumping power increases to 7.78 μW, 12 clear lasing modes with the full width at half-maximum (fwhm) of about 0.036 nm can be distinguished in the emission spectrum for the strongest resonant peak located at 393.39 nm, so the Q factor is estimated as 10925 according to the definition $Q = \lambda/\Delta\lambda$, where λ and $\Delta\lambda$ are the peak wavelength and the fwhm, respectively. For the Al-decorated ZnO microrod, some sharp peaks emerge out when the pumping power reaches to 2.15 μW. As the pumping power increases to 3.67 μW, 16 clear lasing modes with the fwhm of about 0.13 nm can also be distinguished in the emission spectrum. The mode spacing is as the same as that of the bare ZnO one, and the strongest resonant peak is located at 393.25 nm. The Q factor is about 3025, which is smaller than that of the bare ZnO microrod due to the scattering of Al NPs. In order to further analyze the action of the Al NPs to the enhancement of ZnO WGM lasing, the lasing spectra from the two samples with and without Al

dx.doi.org/10.1021/ph5002582 | ACS Photonics 2015, 2, 73−77

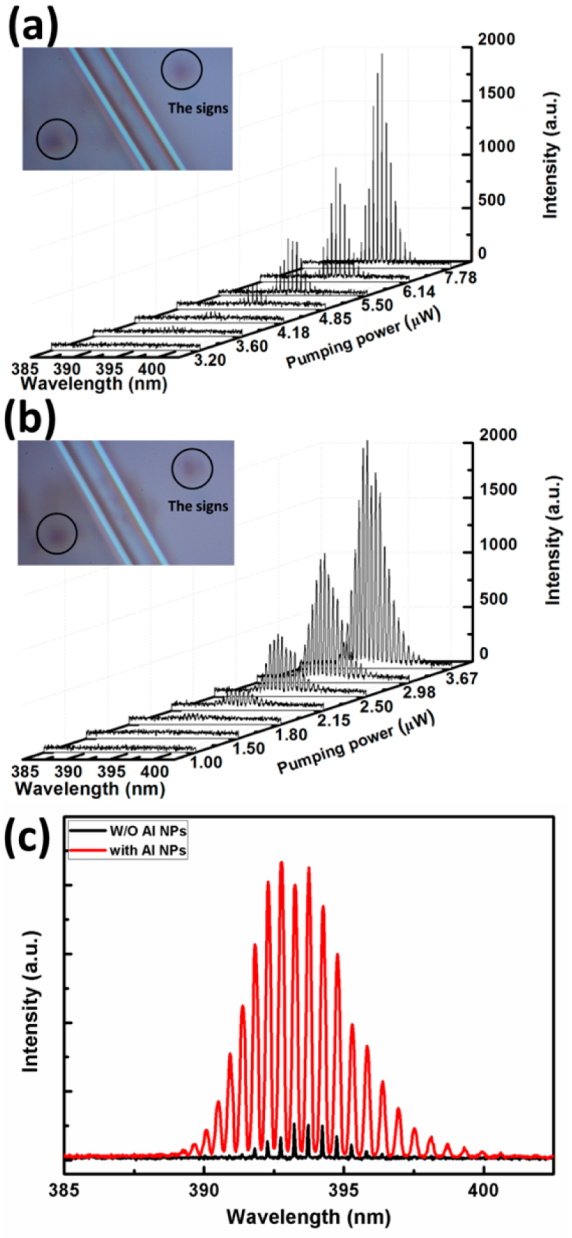

Figure 4. Lasing spectra of an individual ZnO microrod (a) before and (b) after Al NPs decoration under different pumping power. (c) The lasing spectra for the two samples under the same excitation power of 5.5 μW. Inset shows the optical microscopy images of the individual ZnO microrod before and after Al NPs decoration.

NPs decoration under the same pumping power of 5.5 μW were compared, as shown in Figure 4c. The enhancement ratio of lasing intensity was more than 8-fold when ZnO microrod was decorated with Al NPs. It is worth noting that, in Figure 4c, a slightly blue-shift of the envelope of lasing emission peaks which is corresponding to the spontaneous emission was also observed after depositing Al NPs on the surface of the ZnO microrod. The reason can also be attributed to the strong resonant surface plasmon coupling between ZnO microrod and Al NPs as mentioned before. Hence, the significant benefit composited with metal NPs is that it can immensely enhance the performance of the optical microcavity by the SPR coupling between the metal NPs and semiconductor micro/nanostructures.

Figure 5 shows the integrated emission intensity versus excitation power from the two samples. For the bare ZnO

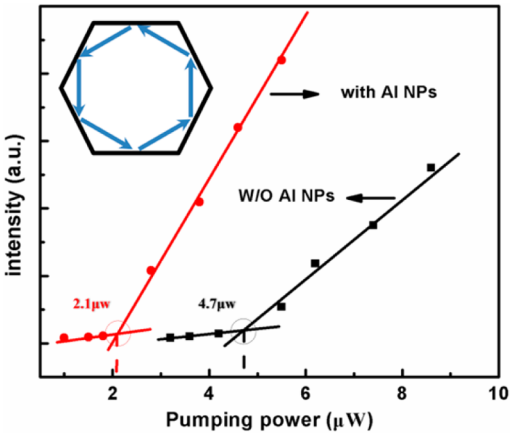

Figure 5. Dependence of the emission intensity on the pumping power. The inset shows the optical path in the hexagonal WGM cavity.

microrod, the emission intensity increases slowly under the excitation power of 4.7 μW and it increases rapidly when the excitation power is higher than 4.7 μW. This indicates that the lasing threshold is about 4.7 μW for the bare ZnO microrod. Quite interestingly, the threshold of the ZnO microrod decorated with Al NPs (2.1 μW) reduces significantly compared with that of bare one (4.7 μW), which means that the laser action can be more easily achieved in the ZnO microrod/Al NPs composite system. Based on the coupling mechanism mentioned above, the reduced threshold provides additional evidence to support the energy coupling between ZnO microrod and Al NPs.

CONCLUSIONS

To summarize, we provide a novel approach to enhance lasing performance from a semiconductor WGM optical microcavity based on metal−semiconductor SPR coupling. To illustrate the working principle, ZnO microrod decorated with Al NPs was chosen as an example. More than 10-fold enhancement of the spontaneous and stimulated emission was observed due to the result of strong resonant surface plasmon coupling between ZnO microrod and Al NPs. In addition, compared to the bare ZnO microrod, the threshold of the microcavity with Al NPs decoration has been cut in half relative to the case without Al NPs. This approach can be extended to a variety of metal−semiconductor composite systems for designing of novel optoelectronic devices with high efficiency.

EXPERIMENTAL SECTION

ZnO microrods were synthesized in a horizontal tube furnace through a simple vapor-phase transport process, as our previous report.[29] A mixture of ZnO and graphite powder with mass ratio of 1:1 was filled into a small quartz boat as source material, which was placed in the center of the heating zone, and a silicon slice was covered on the quartz boat. Then, the furnace was heated up to 1150 °C by the heating rate of 10 °C/min. ZnO microrods were obtained on the silicon substrate after reaction for 45 min. The Al NPs were sputtered onto an individual ZnO microrod by radio frequency magnetic sputtering, the chamber pressure was fixed at 2.0 Pa, the Ar flow was 50 sccm, the sputtering power was 100 W, and the sputtering procedure

dx.doi.org/10.1021/ph5002582 | ACS Photonics 2015, 2, 73−77

lasted for 5 min. In order to ensure the lasing spectra collected from the same emission region, two artificial signs were marked by the femtosecond pulsed laser at both sides of the ZnO microrod before decorating with Al NPs, as shown in the inset in Figure 4a,b. The morphology of the samples was observed by optical microscope (OLYMPUS BX53F) and a field emission scanning electron microscopy (FESEM, Carl Zeiss Ultra Plus) equipped with an X-ray energy dispersive spectrometer (EDS) (Oxford X-Max 50). The absorption measurement was carried out by UV−vis-NIR spectrophotometer (SHIMADZU UV-2600). The microphotoluminescence (μ-PL) and lasing spectra from an individual ZnO microrod was measured by a confocal μ-PL system (OLYMPUS BX53) coupled with a femtosecond pulsed laser at 325 nm (COHERENT Libra-F-HE) as the excitation source. All measurements were performed at room temperature.

AUTHOR INFORMATION

Corresponding Author

*E-mail: xcxseu@seu.edu.cn.

Notes

The authors declare no competing financial interest.

ACKNOWLEDGMENTS

This work was supported by "973" Program (2011CB302004 and 2013CB932903), NSFC (61275054, 61475035, 11104119, and 11404289).

REFERENCES

(1) Tsukazak, A.; Ohtomo, A.; Onuma, T.; Makoto, O.; Makino, T.; Sumiya, M.; Ohtani, K.; Chichibu, S. F.; Fuke, S.; Segawa, Y.; Ohno, H.; Koinuma, H.; Kawasaki, M. Repeated Temperature Modulation Epitaxy for p-Type Doping and Light-Emitting Diode Based on ZnO. *Nat. Mater.* **2005**, *4*, 42−46.

(2) Yang, Q.; Wang, W. H.; Xu, S.; Wang, Z. L. Enhancing Light Emission of ZnO Microwire-Based Diodes by Piezo-Phototronic Effect. *Nano Lett.* **2011**, *11*, 4012−4017.

(3) Lupan, O.; Pauporté, T.; Viana, B. Low-Voltage UV-Electroluminescence from ZnO-Nanowire Array/p-GaN Light-Emitting Diodes. *Adv. Mater.* **2010**, *22*, 3298−3302.

(4) Xu, S.; Xu, C.; Liu, Y.; Hu, Y. F.; Yang, R. S.; Yang, Q.; Ryou, J. H.; Kim, H. J.; Lochner, Z.; Choi, S.; Dupuis, R.; Wang, Z. L. Ordered Nanowire Array Blue/Near-UV Light Emitting Diodes. *Adv. Mater.* **2010**, *22*, 4749−4753.

(5) Huang, M. H.; Mao, S.; Feick, H.; Yan, H.; Wu, Y. Y.; Kind, H.; Weber, E.; Russo, R.; Yang, P. D. Room-Temperature Ultraviolet Nanowire Nanolasers. *Science* **2001**, *292*, 1897−1899.

(6) Chu, S.; Wang, G. P.; Zhou, W. H.; Lin, Y. Q.; Chernyak, L.; Zhao, J. Z.; Kong, J. Y.; Li, L.; Ren, J. J.; Liu, J. L. Electrically Pumped Waveguide Lasing from ZnO Nanowires. *Nat. Nanotechnol.* **2011**, *6*, 506−510.

(7) Dai, J.; Xu, C. X.; Sun, X. W. ZnO-Microrod/p-GaN Heterostructured Whispering- Gallery-Mode Microlaser Diodes. *Adv. Mater.* **2011**, *23*, 4115−4119.

(8) Chu, S.; Olmedo, M.; Yang, Z.; Kong, J. Y.; Liu, J. L. Electrically Pumped Ultraviolet ZnO Diode Lasers on Si. *Appl. Phys. Lett.* **2008**, *93*, 181106.

(9) Soci, C.; Zhang, A.; Xiang, B.; Dayeh, S. A.; Aplin, D.; Park, J.; Bao, X. Y.; Lo, Y. H.; Wang, D. ZnO Nanowire UV Photodetectors with High Internal Gain. *Nano Lett.* **2007**, *7*, 1003−1009.

(10) Yang, Q.; Guo, X.; Wang, W. H.; Zhang, Y.; Xu, S.; Lien, D. H.; Wang, Z. L. Enhancing Sensitivity of a Single ZnO Micro-/Nanowire Photodetector by Piezo-Phototronic Effect. *ACS Nano* **2010**, *4*, 6285−6291.

(11) Fu, X. W.; Liao, Z. M.; Zhou, Y. B.; Wu, H. C.; Bie, Y. Q.; Xu, J.; Yu, D. P. Graphene/ZnO Nanowire/Graphene Vertical Structure Based Fast-Response Ultraviolet Photodetector. *Appl. Phys. Lett.* **2012**, *100*, 223114.

(12) Hassan, J.; Mahdi, M.; Kasim, S.; Ahmed, N. M.; Abu Hassan, H.; Hassan, Z. High Sensitivity and Fast Response and Recovery Times in a ZnO Nanorod Array/p-Si Self-Powered Ultraviolet Detector. *Appl. Phys. Lett.* **2012**, *101*, 261108.

(13) Cao, H.; Zhao, Y. G. Random Laser Action in Semiconductor Powder. *Phys. Rev. Lett.* **1999**, *82*, 2278−2281.

(14) Czekalla, C.; Sturm, C.; Schmidt-Grund, R.; Cao, B. Q.; Lorenz, M.; Grundmann, M. Whispering Gallery Mode Lasing in Zinc Oxide Microwires. *Appl. Phys. Lett.* **2008**, *92*, 241102.

(15) Sun, L. X.; Chen, Z. H.; Ren, Q. J.; Yu, K.; Bai, L. H.; Zhou, W. H.; Xiong, H.; Zhu, Z. Q.; Shen, X. C. Direct Observation of Whispering Gallery Mode Polaritons and their Dispersion in a ZnO Tapered Microcavity. *Phys. Rev. Lett.* **2008**, *100*, 156403.

(16) Ru1hle, S.; Vugt, L. K. van; Li, H. Y.; Keizer, N. A.; Kuipers, L.; Vanmaekelbergh, D. Nature of Sub-Band Gap Luminescent Eigenmodes in a ZnO Nanowire. *Nano Lett.* **2008**, *8*, 119−123.

(17) Zhang, S. G.; Zhang, X. W.; Yin, Z. G.; Wang, J. X.; Si, F. T.; Gao, H. L.; Dong, J. J.; Liu, X. Optimization of Electroluminescence from n-ZnO/AlN/p-GaN Light-Emitting Diodes by Tailoring Ag Localized Surface Plasmon. *J. Appl. Phys.* **2012**, *112*, 013112.

(18) Chu, S.; Ren, J. J.; Yan, D.; Huang, J.; Liu, J. L. Noble Metal Nanodisks Epitaxially Formed on ZnO Nanorods and Their Effect on Photoluminescence. *Appl. Phys. Lett.* **2012**, *101*, 043122.

(19) Cheng, C. W.; Sie, E. J.; Liu, B.; Huan, C. H. A.; Sum, T. C.; Sun, H. D.; Fana, H. J. Surface Plasmon Enhanced Band Edge Luminescence of ZnO Nanorods by Capping Au Nanoparticles. *Appl. Phys. Lett.* **2010**, *96*, 071107.

(20) Lin, Y.; Xu, C. X.; Li, J. T.; Zhu, G. Y.; Xu, X. Y.; Dai, J.; Wang, B. P. Localized Surface Plasmon Resonance-Enhanced Two-Photon Excited Ultraviolet Emission of Au-Decorated ZnO Nanorod Arrays. *Adv. Opt. Mater.* **2013**, *1*, 940−945.

(21) Wang, C. S.; Lin, H. Y.; Lin, J. M.; Chen, Y. F. Surface-Plasmon-Enhanced Ultraviolet Random Lasing from ZnO Nanowires Assisted by Pt Nanoparticles. *Appl. Phys. Express* **2012**, *5*, 062003.

(22) Oulton, R. F.; Sorger, V. J.; Zentgraf, T.; Ma, R. M.; Gladden, C.; Dai, L.; Bartal, G.; Zhang, X. Plasmon Lasers at Deep Subwavelength Scale. *Nature* **2009**, *461*, 629−632.

(23) Dintinger, J.; Klein, S.; Ebbesen, T. W. Molecule-Surface Plasmon Interactions in Hole Arrays: Enhanced Absorption, Refractive Index Changes, and All-Optical Switching. *Adv. Mater.* **2006**, *18*, 1267−1270.

(24) Huang, X. H.; Ei-sayed, I. E.; Qian, W.; Ei-sayed, M. A. Cancer Cells Assemble and Align Gold Nanorods Conjugated to Antibodies to Produce Highly Enhanced, Sharp, and Polarized Surface Raman Spectra: A Potential Cancer Diagnostic Marker. *Nano Lett.* **2007**, *7*, 1591−1597.

(25) Zhang, S. G.; Zhang, X. W.; Yin, Z. G.; Wang, J. X.; Dong, J. J.; Gao, H. L.; Si, F. T.; Sun, S. S.; Tao, Y. Localized Surface Plasmon-Enhanced Electroluminescence from ZnO-Based Heterojunction Light-Emitting Diodes. *Appl. Phys. Lett.* **2011**, *99*, 181116.

(26) Dai, J.; Xu, C. X.; Zheng, K.; Lv, C. G.; Cui, Y. P. Whispering Gallery-Mode Lasing in ZnO Microrods at Room Temperature. *Appl. Phys. Lett.* **2009**, *95*, 241110.

(27) Ekinci, Y.; Solak, H. H.; Löffler, J. F. Plasmon Resonances of Aluminum Nanoparticles and Nanorods. *J. Appl. Phys.* **2008**, *104*, 083107.

(28) Chan, G. H.; Zhao, J.; Schatz, G. C.; Van Duyne, R. P. Localized Surface Plasmon Resonance Spectroscopy of Triangular Aluminum Nanoparticles. *J. Phys. Chem. C* **2008**, *112*, 13958−13963.

(29) Zhu, G. P.; Xu, C. X.; Zhu, J.; Lv, C. G.; Cui, Y. P. Two-Photon Excited Whispering-Gallery Mode Ultraviolet Laser from an Individual ZnO Microneedle. *Appl. Phys. Lett.* **2009**, *94*, 051106.

(30) Lawrie, B. J.; Haglund, R. F., Jr; Mu, R. Enhancement of ZnO Photoluminescence by Localized and Propagating Surface Plasmons. *Opt. Express* **2009**, *17*, 2565−2572.

(31) Wang, X. D.; J. Summers, C.; Wang, Z. L. Large-Scale Hexagonal-Patterned Growth of Aligned ZnO Nanorods for Nano-optoelectronics and Nanosensor Arrays. *Nano Lett.* **2004**, *4*, 423−426.
(32) Xu, X. Y.; Xu, C. X.; Lin, Y.; Ding, T.; Fang, S. J.; Shi, Z. L.; Xia, W. W.; Hu, J. G. Surface Photoluminescence and Magnetism in Hydrothermally Grown Undoped ZnO Nanorod Arrays. *Appl. Phys. Lett.* **2012**, *100*, 172401.
(33) Michaelson, H. B. The Work Function of the Elements and its Periodicity. *J. Appl. Phys.* **1977**, *48*, 4729−4733.
(34) Skriver, H. L.; Rosengaard, N. M. Surface Energy and Work Function of Elemental Metals. *Phys. Rev. B* **1992**, *46*, 7157−7168.